A Case for Feedback Control to Prevent Delay

Paul J. Ossenbruggen Member, ASCE[1]

[1]Department of Civil Engineering, University of New Hampshire, Durham NH 03824.

Email: pjo@unh.edu

ABSTRACT

A field experiment was conducted at a site with no bottleneck. Traffic delay in the form moving queues was observed. The only explanation, according to the authors, was the drivers inability to maintain a constant speed. The variability in speed data is called "traffic volatility." This experiment served as motivation to: (1) explain traffic delay with Brownian motion and car following modeling; and (2) by theoretically assuming all vehicles are equipped with a smart technology device, can prevent traffic delay by using Kalman Filter feedback control. Feedback control proved to be effective tool. Its effectiveness is demonstrated by using (simulated) delay data as input to the Kalman Filter model and showing that all vehicles can effectively track a target speed, thereby minimize traffic volatility. The delay data are obtained by using two steps. First, data of a diverse set of drivers, ranging from risk averse to aggressive, are simulated with a Brownian motion model. Second, these data are input into a car following model that can detect unsafe driving conditions. If an unsafe condition is detected, then the following vehicle's speed is reduced and gap between the lead and following vehicles is adjusted for safety. Traffic performance is measured with average group speed and with traffic density and flow estimates. Thus, estimates from the delay and feedback control models can be compared. The approach is critiqued and the practically of using a feedback control system at a bottleneck is presented.

Keywords: Traffic breakdown, car following, congestion, control, intelligent systems, stochastic processes

INTRODUCTION

Sugiyama et al. (2008) team conducted a simple but eloquent field experiment around a single-lane roadway. We call it a "ring-road" experiment. The research team instructed drivers to accelerate to a constant speed and then maintain that speed, a target speed u^*. At the start of the experiment, the vehicles were evenly spaced at a known distance, measured as a target headway s^*. The drivers were unable to maintain speed u^* or headway s^* (Villatoro 2019). Soon after the initiation of the experiment, moving queues were observed. Seconds later, some vehicles stopped momentarily and started up again. The system was unstable because the distance between vehicles, expressed as a traffic density $k^* = 1/s^*$, was sufficiently high to allow small perturbations in speed to cause delay, "to show the emergence of a jam with no bottleneck."

If the vehicles in the "ring-road" experiment were outfitted with some smart technology or ITS (intelligent transportation system) device, can moving queues and delay be prevented? Given the advances in hardware and software suggests the answer should be "Yes."

This paper uses a "thought" experiment to answer this challenging question. The approach uses one mathematical model that simulates field conditions and a second model that tests the effectiveness of the method. Brownian motion model data, which is fed into a car following model, is developed to simulate the "ring-road" experiment. A feedback control model is used to evaluate the effectiveness of the method in preventing moving queue formation. Brownian-motion/car-following model data are used as input to a Kalman Filter feedback control model. The claim is: By controlling speed u, it is sufficient to control s^* and k^*, to minimize the perturbations in speed, and to prevent delay. In this paper, the "small perturbations in speed" are called *traffic volatility*, which is denoted as σ. In summary, by controlling speed, $u \to u^*$, leads to controlling $s \to s^*$, $k \to k^*$ and minimizing $\sigma \to 0$. Controlling u also leads to performance benefits. If true, traffic flow can reach a maximum flow $q^* = u^* \cdot k^*$ or possibly exceed it without queuing, delay or traffic breakdown. The aim of this paper is to offer evidence that this claim have a good chance of succeeding.

Efforts are made to show that the mathematical models chosen for this study can explain and identify the conditions that lead to queuing and delay. The chance of traffic breakdown is high when the traffic demand q approaches or exceeds roadway capacity c, or $q \simeq c$. The Highway Capacity Manual (TRB 2010) is used to assign the target values u^* and $s^* = 1/k^*$ in our analysis. The average flow at capacity for a single freeway lane is $c = \bar{q} =$ 2,380 v/h where $\bar{k} = 28$ $passenger - cars/km/lane$ (45 $pc/mile/lane$), $\bar{u} = 85$ km/h (53 mph). Thus, delay is expected when $u = \bar{u}$ and $s = 1/\bar{k}$ are assigned as model inputs. Since the drivers in the simulated "ring-road" experiment are under stress, the flow under this condition is expected to be less than capacity, $q < c$.

Simulating the Sugiyama team "ring-road" experiment has a major advantage. No question that the simple road geometry used in the field experiment made the importance of traffic volatility σ easier to identify. This study also takes advantage of a single traffic lane.

The paper is organized as follows. The **Notation** section contains a list of model parameters and variables sorted by model class. The **Methods** section describes the important features of the Brownian motion and Kalman Filter feedback control models. The **Analysis** section includes a problem definition and descriptions of individual driver behavior, a "rule of the road" for safe driving definition, and things that affect the drivers operating vehicles at roadway capacity. Naturally, modeling queuing and estimating traffic performance - speed, density and flow - and Kalman Filter feedback control are discussed. A *car-following algorithm* is described here. The **Discussion** section contains a critique of the "ring road" experiment and a discussion for developing a feedback control system with practical application at a bottleneck.

Readers are urged to peruse the tables and figures and take note that time-speed $t - \dot{x}$ and time-space $t - x$ trajectories are used extensively to give a reader an intuitive feel of this complicated process. The computer code used in the development of this paper is freely available (Ossenbruggen 2019).

METHODS

Every attempt is made to capture reality. For this study, we focus our modeling efforts on an individual driver and how each react when driving in the "ring road" *car-following* experiment. For example, a driver will brake to avoid crashing into a vehicle in front of it. The braking behavior depends on the type of vehicle that the person is driving. This feature as well as others are introduced into the analysis and will be introduced into the discussion presently.

A Kalman Filter Feedback Control Model

Feedback control is a recursive procedure: a data point is collected and then is used to forecast the next state. A Kalman filter of a linear system is expressed as:

$$\frac{d}{dt}\mathbf{x} = \mathbf{A}\mathbf{x} + \mathbf{B}\mathbf{u} + \mathbf{w}_d \tag{1}$$

$$\mathbf{y} = \mathbf{C}\mathbf{x} + \mathbf{D}\mathbf{u} + \mathbf{w}_n \tag{2}$$

where the matrices $\mathbf{x}$ and $\mathbf{u}$ for the "ring-road" experiment are $\mathbf{x} = dx/dt = \dot{x}$ for vehicle speed, and $\mathbf{u} = f$ for force. Excellent sources of information about feedback control are contained in the writings of Durbin and Koopman (2012) and Anderson and Moore (1979). For feedback control, the writings of Doyle et al. (1992) and Duriez et al. (2017) are recommended.

Substituting $\mathbf{w_d} = \mathbf{w_n} = \mathbf{D} = 0$ (MATLAB@9.2 2019), the stochastic model reduces to a deterministic model of the form:

$$\ddot{x} = \left(\frac{-f_d}{m}\right)\left(\dot{x}\right) + \left(\frac{1}{m}\right)\left(f\right) \tag{3}$$

$$y = \left(1\right)\left(\dot{x}\right) \tag{4}$$

where $\ddot{x}$ is vehicle acceleration, $\mathbf{x} = \mathbf{y} = \dot{x}$, and $\mathbf{u} = f$. The drag force f_d term, estimated using a first-order Taylor-series expansion, is derived from the nonlinear equation, $f_d = \rho \cdot C_d \cdot A \cdot u^2/2$ where ρ is the air density, C_d is the vehicle drag coefficient, A is the frontal area of the vehicle, and u is vehicle speed. All drivers, who are assumed to be driving an average American passenger vehicle, will accelerate by applying force $\mathbf{u} = f$. The drag force is estimated to be equal to $f_d = 212\ N$ ($48\ lb$) when traveling at $\bar{u} = 85\ km/h$ ($53\ mph$).

The reader should be aware that u and $\dot{x}$ notation both denote speed. The u notation is typically used when referring mechanistic functions, such as given in the preceding paragraph, and to targets as given in the **Introduction**. The $\dot{x}$ notation is generally used when referring to model forecasts, simulated data, and $t - \dot{x}$ trajectories as given in the next paragraph.

Simulating with equations 1 and 2, a time-velocity $t - \dot{x}$ trajectory shown in the upper panel of Figure 1 is obtained. According to the model, a driver will accelerate very slowly. Drivers, of course, don't drive this way. The forecast is nonsense. By applying LQR feedback control to the model, a driver will accelerate at a comfortable rate to reach the target speed u^*, as shown in the lower panel, as a $t - \dot{x}$ trajectory. *Since this trajectory plays an important role in this paper, it is treated as a target and given the following notation:* $t - u^*$. Its importance will be illustrated most profoundly in the **Feedback Control** section.

A LQR (Linear Quadratic Regulator) minimizes the control effort (Duriez et al. 2017). Control effort is defined as the costs associated with the deviation from the target state plus the cost associated with reaching the target state. These costs are introduced into a quadratic cost function and minimized. A comfortable acceleration rate is found by trial and error. By the way, the LQR model plays an important role in feedback control, but it is not a Kalman Filter control model.

Brownian Motion Model

Stochastic differential equations (SDEs) consist of two components; a deterministic and a stochastic component. A Brownian motion model, a class of SDE, is expressed as:

$$dX = \mu \cdot dt + \sigma \cdot dW \tag{5}$$

where the deterministic and stochastic components are $\mu \cdot dt$ and $\sigma \cdot dW$, respectively. Time t is treated as a continuous variable and W denotes *Brownian motion.* The solution to this time-series model can be expressed as:

$$X_t = x_0 + \mu \cdot t + \sigma \int_0^t dW, \qquad t \geq 0 \tag{6}$$

where x_0 is the initial state at time $t = 0$.

In lieu of solving the stochastic integral or Itô integral, we will treat (5) as a discrete system and obtain a solution using simulation (Iacus 2008) Maybeck (1979). The stochastic integral is simulated as $W(\Delta t) \sim \sqrt{\Delta t} \cdot N(0, 1)$ where $N(0, 1)$ represents a standard Normal distribution. Δt replaces dt. Eq(6), expressed on a discrete time scale, is:

$$X_\kappa = X_{\kappa-1} + \mu \cdot \Delta t + \sigma \cdot W(\Delta t) \tag{7}$$

where subscript κ is the time-step index at t. In our application, the response variable X, a random variable, denotes vehicle location. Thus, it is useful to think of X_k as an one-step ahead Δt *forecast* location at κ where X_{k-1} is an *observed* location at $\kappa - 1$. Using a finite difference approximation, speed at time κ is estimated as:

$$\dot{X}_\kappa = \frac{X_\kappa - X_{\kappa-1}}{\Delta t} \tag{8}$$

The simulation results presented in this paper use a time-step of $\Delta t = 0.1$ second and a time range from 0 to 60 seconds. Time on the discrete scale is denoted as $\kappa = 0, 0.1, 0.2, \ldots, 60$ seconds.

ANALYSIS

The Sugiyama team used more than twenty vehicles in their field study. In our computer simulation study, four vehicles are used. There are two reasons for this choice. One, it avoids graphical clutter. Second, the "small perturbations in speed causing breakdown" comment made above suggests the individual driver causes breakdown. Therefore, limiting the investigation of driving behavior to four drivers is for clarity.

Each driver is assumed to have an unique driving style as shown in Table 1. The values of $u = \dot{x}$ are the *speeds the driver's wish* to obtain if unimpeded. Again for simplicity in presentation, driver 1 operates the lead vehicle. Thus by definition, this vehicle is unimpeded. The $\hat{s}$ values are the safe space headway values for these speeds. At the start of the experiment at time $\kappa = 0$, all vehicles are equally spaced at a distance of three passenger car lengths, s_0.

Individual Drivers

For the present, the focus is on one driver, the driver of vehicle 2. At a speed of $\mu = 21\ m/s$ ($70\ fps$), this person wishes to drive at a speed less than the target speed $u^* = 23.7\ m/s$. In the "ring-road" experiment, σ values are assigned to reflect a driver's ability to follow instructions. Driver 2 is given a $\sigma = 0.61\ m/s$ ($2.0\ fps$) assignment and is described to be an "average" driver.

To appreciate these assignments, we will contrast them against a driver, who is judged to be a reckless, risk-taker. He is observed driving well above the posted speed limit of 29 m/s (65 mph) on a multiple lane freeway and darting around slower moving vehicles, at speeds ranging from 31 to 40 m/s (70 to 90 mph). Assuming that his speed range lies within a 95% confidence interval, we can estimate the standard deviation, which we call σ_{max}. We estimate it to be 2.2 m/s (5 mph). The most "inattentive" driver in our study is driver 1 with an assignment of $\sigma = 1.22\ m/s$ ($4\ mph$). In addition, since this individual prefers to drive in excess of u^*, the driver is described as an "aggressive driver." This subjective assignment method is used to describe the other drivers in the experiment.

The effects of the u and σ assignments on the experiment can been seen in Figure 2. Concentrate on drivers 1 and 3. Their speed profile, shown in the top panel as a time-speed

$t - \dot{x}$ trajectory, show them to accelerate more aggressively than the other drivers. Driver 1 reaches a speed of $u = 38\ m/s$ ($85\ fps$) in 10 seconds, which is considered a comfortable acceleration rate.

Now, concentrate on drivers 2 and 3 in the middle panel. Driver 2, described as an "average driver," impedes the progress of driver 3. Notice that all simulated trajectories shown in the figure use output from the LQR feedback model (3) and Brownian motion model (7). All $t - x$ trajectories are relatively smooth regardless of the fact, the $t - \dot{x}$ trajectories are not. This effect is directly related to traffic volatility σ. The time-distance $t - x$ trajectories for drivers 2 and 3 cross, which indicates a crash. Of course, it is not permissible in our "ring-road" experiment. The problem of crossing $t - x$ trajectories will be addressed in the next section on car-following and the solution to this problem will be incorporated into a *car-following algorithm.*

The vehicle arrival order is vitally important. If the fastest vehicle arrived first and the slowest one last with a vehicle arrival order of 1, 3, 2 and 4, then one could claim that there is no conflict, no crashes, no near-misses and no delay. That claim is true only if the traffic volatility σ is zero for all vehicles. Granted it is difficult to visualize the impact of Brownian motion in the middle and lower panels of Figure 2; but most assuredly, it is playing a role.

Group Behavior and Car-Following

In this study, all drivers are law abiding and all follow a "rule of the road" for maintaining a safe headway. Traffic density $k = 1/s$ is equally important as is the vehicle arrival order. It is also an important traffic performance measure. The effect of k and s can be visualized by comparing the $t - x$ trajectories of the middle and lower panels of Figure 2. The traffic headway shown in middle panel is four-times greater than the one in the lower panel. By definition, it has a traffic density one-fourth of the one in the lower panel. Thus, the traffic in the middle panel is considered to be light with a small chance of delay.

Light traffic is no guarantee that traffic will not be delayed. Observe the vehicle trajectory crossings in the lower panel occur sooner than those in the middle panel. For example, the trajectory crossing times for vehicles 2 and 3 occur at around $\kappa = 30$ seconds in the middle panel and at a time κ less than 10 seconds in the lower panel. In other words, the potential for crossing trajectories can occur during acceleration. Our *car-following algorithm* is designed to account for this fact.

The algorithm is also designed to account for the fact that all "ring-road" experiment drivers are safe drivers. They follow the "rule of the road" lesson taught in American driving schools. The rule is: *a driver should maintain a distance of at least one vehicle length for each 10 mph driven.* This rule was applied to obtain the $\hat{s}$ values in Table 1.

The Car-Following Algorithm

The books by Elefteriadou (2014) and Trieber and Kesting (2013) contain a comprehensive collection and descriptions of car-following algorithms used for a wide variety of applications including lane changing and gap acceptance. The one described here is similar in concept to ones described in these books. The one developed here takes advantage of the simple mathematical structure of the Brownian motion model and also attempts to capture the effects of human behavior on performance (Hamdar et al. 2015).

The *car-following algorithm* uses the following steps: (1) The safe headway distance is determined for each time step of $\kappa = 0, 0.1, 0.2, \ldots, 60$ seconds for lead vehicle L as $\hat{s}^*_\kappa = f(u_L, l)$. (2) The distance headway for the following vehicle F is estimated, $s_k = x_{L,\kappa} - x_{F,\kappa}$. (3) Violation times are identified. If $s_\kappa < \hat{s}^*_\kappa$, then the time κ is stored in κ^*. (4) For all $\kappa \in \kappa^*$, (a) the following vehicle speed is reduced to the lead vehicle speed, $u_{F,\kappa} = u_{L,\kappa}$; and (b) a revised following vehicle location is determined, $x_{F,\kappa} = x_{L,\kappa} - \hat{s}^*_\kappa$.

The car-following speed, headway and travel distance effects on vehicles 2 and 3 are shown in Figure 3. The driver of vehicle 2 is designated by the subscript L for lead vehicle. Vehicle 3 is designated by F for being a following vehicle. The speeds of vehicle 2 and 3 are the same for $\kappa > 3$ seconds. Within seconds of start up, driver 2 decelerates to avoid a crash. The lower panel shows the $t - x$ trajectories for the two drivers no longer cross one another. The two vehicles are traveling safely. They form a moving queue.

Owing to vehicle arrival times and their driving styles, the drivers of vehicle 1 and 4 are not affected by the queue. The lower panel of Figure 2 show their progress to be unimpeded.

Traffic Performance

Traffic performance measures of speed, density and flow are estimated as time series averages (Vandaele 1983):

$$\bar{u}_\kappa = \frac{1}{n}\sum_{i=1}^{n} u_{i,\kappa} \tag{9}$$

$$\bar{k}_\kappa = \frac{1}{n}\sum_{i=1}^{n} k_{i,\kappa} \tag{10}$$

$$\bar{q}_\kappa = \bar{u}_\kappa \cdot \bar{k}_\kappa \tag{11}$$

where $i = 1, 2, 3, 4$ are the driver numbers given in Table 1. The speeds $u_{i,\kappa}$ and $k_{i,\kappa}$ are output from the *car-following algorithm* for time-steps $\kappa = 0, 0.1, 0.2, \ldots, 60$ seconds.

The time series of Figure 4 brings clarity to reporting the group performance of the four "ring road" vehicles. Each driver's behavior is summarized in Table 2. After accelerating or when $\kappa > 10$ seconds, the mean speed of the four vehicles remain constant and the traffic density and flow decline with time. The average speed is less than the target speed $u^* = 23.7$ m/s (53 mph): $\bar{u} = 21.8$ km/h (48.8 mph) for $10 < \kappa \leq 60$ seconds. A lose in performance claim can be made about the flow. At $\kappa = 60$ seconds, $\bar{q}_{60} = 1{,}600$ vph when the target is $q^* = 2{,}380$ vph. It is also revealing to learn that traffic density is decreasing with time. This evidence supports the notion that the loss in performance rests mainly on driver 2. *The root cause of performance loss has been identified.*

The graphs used throughout this paper are aimed at giving the reader an intuitive feel of the process. Often, they reveal some important fact. However, relying exclusively on visual inspection can be misleading. Consequently, some important underlying feature or fact may be not revealed. Care must be exercised with time series. As such, the *car-*

following algorithm uses a Box-Jenkins modeling method to guard against this oversight. For our purposes, we want to declare if a time series is stationary or nonstationary. The method uses autocorrelation and partial autocorrelation statistics to fit an ARIMA model and then tests the model parameters for statistical significance. For $\kappa > 10$ seconds, the $\bar{u}_\kappa$ times series is declared stationary because (1) its variance is judged to be constant and (2) there are no significant parameters in its ARIMA model. The $\bar{k}_\kappa$ and $\bar{q}_\kappa$ times series are declared nonstationary because (1) their variances are judged to be constant but (2) there are significant parameters in their ARIMA models. These analyses give assurance that there is no trend in the $\bar{u}_\kappa$ times series and there are trends in the $\bar{k}_\kappa$ and $\bar{q}_\kappa$ times series. When the variances are not constant over time and show a trend, the effect has be removed to obtain a clear picture of the series. This step is not necessary in this case because the variances of the $\bar{k}_\kappa$ and $\bar{q}_\kappa$ series are judged to be constant. As such, the analysis gives assurances that vehicles 2 and 3 have formed a moving queue and the driver of vehicle 2 is responsible for the performance loss.

Recall, there are twenty plus vehicles in the "ring road experiment. To simplify the discussion, we focused on four drivers and designated driver 1 as leader. In the Sugiayama team experiment, there was no lead vehicle. All drivers played duel roles as leaders and followers. Moving queues were quickly formed and just as quickly dissipated. Consequently, the "blame" should not rest on an individual driver, but on the group.

Feedback Control

Figure 5 shows the effectiveness of the Kalman Filter feedback control model. The stochastic process described above has been transformed from a disorderly one to an orderly one. Each vehicle tracks the target $t - u^*$ trajectory. To achieve benefits, all vehicles are assumed to be equipped with smart technology. In other words, *all drivers have agreed to relinquish the operation of their vehicles.* Technology takes over.

Table 3 gives another perspective of the effectiveness of the Kalman Filter feedback control model. Compare the "ring road" input $\mathbf{w}$ estimates against the output $\mathbf{y}$ estimates.

The $\mathbf{w}$ input $\bar{u}$ averages have shifted to $\mathbf{y}$ output $\bar{u}$ averages. The simulation indicates that all vehicles on the controlled "ring road" travel at average speed in close proximity to the target u^* speed. The traffic volatility of $\mathbf{y}$ is quite small in comparison to their counterparts of $\mathbf{w}$.

It is worth repeating on how a Kalman Filter functions on an incremental basis over time κ: A data point, $\mathbf{y}$ of equation (2) at time κ, is collected and then the Kalman Filter uses that data point to forecast the next state, $\mathbf{x}$ of equation (1) at time $\kappa+1$. Here are the some details about the Kalman Filter using a third perspective:

1. After a vehicle reaches the target speed u^* at time κ_0, $u_{\kappa_0} = \dot{x}_{\kappa_0} = u^*$, feedback control maintains that speed for all subsequent times, $u_\kappa = \dot{x}_\kappa \to u^*$ for $\kappa > \kappa_0$.
2. The traffic volatility for each vehicle is minimized, $\sigma \to 0$.
3. Each vehicle's $t - x$ trajectory is a straight line. The x location of a vehicle can be estimated as:
$$x_\kappa = x_{\kappa_0} + \bar{u}(\kappa - \kappa_0) + \epsilon, \qquad \kappa > \kappa_0 \tag{12}$$
where $\epsilon \sim N(0, \sigma)$. Equation (12) is valid only for the Kalman Filter feedback control model using estimates, such as those listed under $\mathbf{y}$ of Table 3.
4. The headway between each pair of vehicles is s^*. All vehicles proceed safely.
5. The process has been optimized, the target flow of q^* is obtained.

The group benefits. Delay is prevented.

DISCUSSION

Is smart technology a practical tool for mitigating congestion? Theoretically, by turning over the operation of these vehicles to a smart technology system the goal to prevent delay can be achieved. To be sure, a prototype of the system needs to be tested. If successful, then implementation plans can be made. Lets begin by taking a critical view of the "ring road" experiment.

may be considered an academic exercise that solves a toy problem. Granted, the *car following algorithm* is limited to explaining delay and analyzing performance under special conditions. At the same time, we showed that the importance of traffic volatility σ in explaining delay and demonstrated that its negative effects can be minimized with feedback control: moving queues are eliminated, speeders brought into compliance with the law, and slow pokes and inattentive drivers can be managed to promote operational efficiency. This is a good start but a more challenging problem is needed.

Given the earlier comment, "to show the emergence of a jam with no bottleneck," it is reasonable to study queuing at a bottleneck. For example, when two traffic lanes merge into one, the traffic density doubles and the capacity of a single-lane roadway becomes an issue (Ossenbruggen 2018). Both moving queues and stationary queues can form. Stationary queue wait time, the difference between the arrival and departure rates, becomes an important measure of performance. Drivers entering a bottleneck must be wary of vehicles in front of them and to their side and must make decisions about merging and lane changing. Therefore, mechanistic and SDE models and *car following algorithm* will need to be upgraded.

Regardless, the feedback control model, equations (1) and (2), can address this problem. As with the "ring road" experiment, drivers will start from a standing position, but this time in parallel lanes, accelerate their vehicles to a desired speed, optionally change lanes, and then eventually be forced to merge at the bottleneck. Additional $\mathbf{x}$ data are needed:

- Acceleration $\ddot{x}_{\kappa,lane}$, speed $u = \dot{x}_{\kappa,lane}$, location $x_{\kappa,lane}$, headway $h_{\kappa,lane}$.

where $lane = 1, 2$. It is also important to realize that these observations are measured in seconds, on the micro-scale. Since most traffic studies use fifteen minute vehicle count averages, this is a departure from the norm. The data collection effort is demanding. Regardless, accelerometers, radar, lidar and GPS mounted on and placed in vehicles and on the roadside can gather the needed information (Tarnoff et al. 2009). Communication equipment will allow these data to be shared with individualized "optimized" driver instruction (5G Automotive Association 2018). A stochastic car following model can be implemented (Kendziorra et al. 2016).

The feedback control system envisioned here will be welcomed in a "smart city," a city where different types of sensors (IoT devices) and data manage resources are efficiently used for a wide variety of operations including roadways. The cost to test a feedback system is difficult to estimate but the costs associated with doing nothing are high. For New York State, for example, "The combination of rough roads and congestion costs motorists a total of \$6.3 billion statewide — that's \$694 per driver in NYC, \$504 for Albany, and \$477 for Syracuse" (ASCE 2017). The public need convincing evidence that their tax dollars are used wisely. A Kalman Filter feedback control system was used to put a man on the moon. A good argument can be made that it will work on earth to solve an every day problem.

SUMMARY

Conceptually, a high level of highway performance can be achieved and maintained by using an ITS or smart technology device. The primary objective of the paper is to show that this goal can be achieved with Kalman Filter feedback control. Basically, a two-step approach is used. In step 1, a highway experiment is conducted that shows without control that a traffic delay event occurs: *system failure*. In step 2, using the same data from step 1 and feedback control, traffic delay is prevented: *system success*.

A mechanistic-modeling approach is used to simulate field conditions and explain delay under uncertain conditions. The following lists the most important steps, key features, assumptions and challenges in model building and applying the approach:

- A roadway geometry with one travel lane, a simple "ring road," is used.
- A field experiment where the source uncertainty is easily identified. All drivers promise to maintain a constant target speed u^*. They cannot. The observed speed changes over time. It is called *traffic volatility* σ.

- A “ring road” experiment that simulates field conditions is developed. Traffic delay is highly likely because the traffic flow is set equal to the single lane roadway capacity, $q = c$.
- A simulated “ring road” experiment features individual drivers with different characteristics, ranging from risk averse to aggressive.
- A Brownian motion model that simulates the behavior of each driver.
- A simulated “ring road” delay experiment where the triggering activity is known.
- An evaluation to determine the extent of the delay using time series averages, speed $\bar{u}_\kappa$, density $\bar{k}_\kappa$, and flow $\bar{q}_\kappa$ at times κ.
- An evaluation of the Kalman Filter feedback control model for the above simulation shows delay is prevented and target values of speed u^*_κ, density k^*_κ and flow q^*_κ are obtained.
- The approach is critiqued and the requirements to install a feedback control system at a bottleneck is discussed.

DATA AVAILABILITY STATEMENT

The **MATLAB** code used to perform the analyses described in this paper, including the tables and graphs, are freely accessible from my GitHub website, (Ossenbruggen 2019). No field data are used. Readers may download the code and analyze problems of their own design.

NOTATION

Lower, upper and bold face letters are reserved for constants, random variables and matrices, respectfully. Exceptions are denoted in the body of the paper.

Mechanistic Model: The following list contains performance measures and variables used for deriving a state space model.

f, f_d = force, drag force (N);

g = gravity (m/s^2);

k = density in vehicles per kilometer (v/km);

l = vehicle length (m);

m = vehicle mass (kg);

q = flow in vehicles per hour, (v/h);

s = space headway (m);

w = vehicle weight (N);

x = travel distance (km);

$\dot{x} = u$ = vehicle speed (m/s), (km/h) and

t = time in seconds (s), hours (h).

Stochastic Differential Equations: The Brownian motion model described in the body of the paper is a SDE model.

X = travel distance expressed as a random variable;

$W(\Delta t)$ = Brownian motion or *Wiener Process*;

σ = traffic volatility, expressed as a standard deviation; and

Δt = time-step.

State Space Models:

$\mathbf{x}$ = a vector of state-space variables;

$\mathbf{u}$ = a vector of control variables;

$\mathbf{y}$ = a vector of measured responses of $\mathbf{x}$;

$\mathbf{A}, \mathbf{B}, \mathbf{C}, \mathbf{D}$ = matrices; and

$\mathbf{w_d}, \mathbf{w_n}$ = a disturbance vector, a measurement noise vector;

REFERENCES

5G Automotive Association (2018). "Bridging the Automotive and ICT Industries, <http://5gaa.org/about-5gaa/about-us/>.

Anderson, B. D. and Moore, J. B. (1979). *Optimal Filtering*. Dover.

ASCE (2017). "ASCE Infrastructure Report Card, <https://www.infrastructurereportcard.org>.

Doyle, J. C., Francis, B. A., and Tannenbaum, A. R. (1992). *Feedback Control Theory*. Dover.

Durbin, J. and Koopman, S. J. (2012). *Time Series Analysis by State Space Methods*. Oxford University Press, 2nd edition.

Duriez, T., Brunton, S. L., and Noack, B. R. (2017). *Machine Learning Control - Taming Nonlinear Dynamics and Turbulence*. Springer, 1st edition.

Elefteriadou, L. (2014). *An Introduction to Traffic Flow Theory*. Springer, New York, New York.

Hamdar, S. H., Mahmassani, H. S., and Treiber, M. (2015). "From behavioral psychology to acceleration modeling: Calibration, validation, and exploration of drivers' cognitive and safety parameters in a risk-taking environment." *Transportation Research Part B: Methodological*, 78, 32 – 53.

Iacus, S. (2008). *Simulation and Inference for Stochastic Differential Equations: With R Examples*. Springer-Verlag.

Kendziorra, A., Wagner, P., and Toledo, T. (2016). "A stochastic car following model." *Transportation Research Procedia*, 15, 198 – 207 International Symposium on Enhancing Highway Performance (ISEHP), June 14-16, 2016, Berlin.

MATLAB@9.2 (2019). "Cruise Control: System Modeling, <http://ctms.engin.umich.edu/CTMS/index.php?example=Introduction&section=ControlStateSpace>.

Maybeck, P. S. (1979). *Stochastic Models, Estimation and Control: Volume 1*. Academic Press, Inc.

Ossenbruggen, P. J. (2018). "cartools: Tools for understanding highway performance,

<https://pjossenbruggen.github.io/cartools/index.html>.

Ossenbruggen, P. J. (2019). "cartools: Matlab tools for understanding highway performance, <https://github.com/PJOssenbruggen/cTMATLAB> (April).

Sugiyama, Y., Fukui, M., Kikuchi, M., Hasebe, K., Nakayama, A., Nishinari, K., ichi Tadaki, S., and Yukawa, S. (2008). "Traffic jams without bottlenecks—experimental evidence for the physical mechanism of the formation of a jam." *New Journal of Physics*, 10(3), 033001.

Tarnoff, P., Bullock, D. M., and Young, S. E. (2009). "Continuing evolution of travel time data information collection and processing." *Transportation Research Board Annual Meeting 2009 Paper 09-2030 TRB 88th Annual Meeting Compendium of Papers DVD*, Washington, DC, TRB.

TRB (2010). *Highway Capacity Manual*. Transportation Research Board, National Research Council, Washington, D.C.

Trieber, M. and Kesting, A. (2013). *Traffic Flow Dynamics: Data, Models and Simulation*. Springer.

Vandaele, W. (1983). *Applied Time Series and Box-Jenkins Models*. Academic Press, Inc.

Villatoro, F. (2019). "Traffic jams without bottlenecks—experimental evidence, <https://www.bing.com/videos/search?q=Sugiyama+youtube+traffic&view=detail&mid=8CBD6BA5B1D7F23A1BF38CBD6BA5B1D7F23A1BF3&FORM=VIRE>.

List of Tables

Driver	Description	$u = \dot{x}$ (m/s)	σ (m/s)	$\hat{s}$ (m)	s_0 (m)
1	Aggressive	26	1.22		-
2	Average	21	0.61	20	12.8
3	Slightly Aggressive	24	0.91	23	12.8
4	Risk Averse	20	0.30	19	12.8

TABLE 1. Driver characteristics.

Driver		Headway	Driver
L	F	$\bar{s}$ (m)	F
1	2	-	Leaves queue.
2	3	20	"Tailgates."
3	4	74	Loses ground to queue.

TABLE 2. The effects of car-following.

	Time Series Estimates, $\kappa > \kappa_0$			
	Input: $\mathbf{w}$		Output: $\mathbf{y}$	
Vehicle	$\bar{u}$ (m/s)	σ (m/s)	$\bar{u}$ (m/s)	σ (m/s)
1	25.7	3.6	23.7	0.53
2	21.2	2.0	23.7	0.42
3	21.2	2.0	23.7	0.42
4	19.8	0.95	23.7	0.43

TABLE 3. Kalman Filter feedback control model input and output.

List of Figures

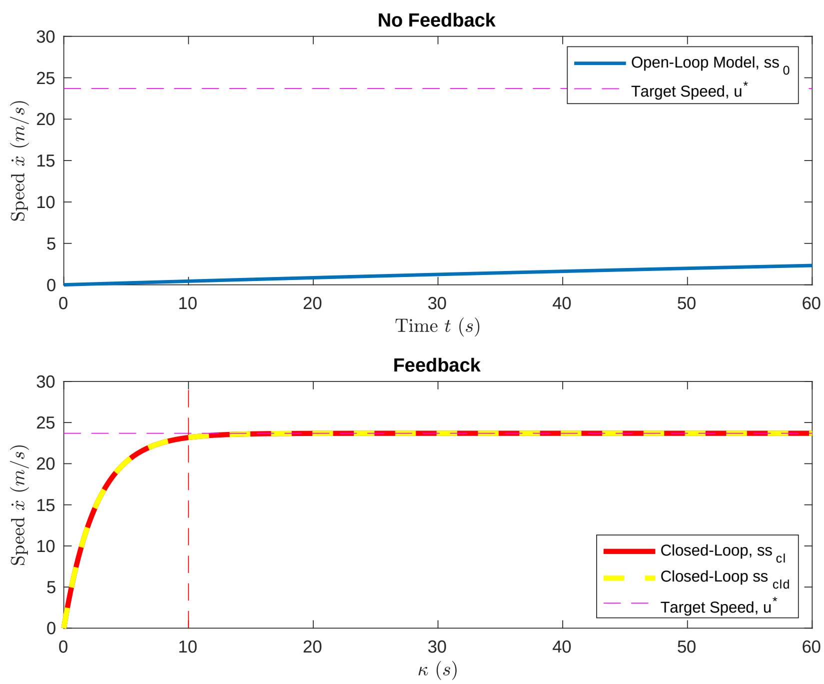

FIG. 1. Mechanistic models for an accelerating vehicle.

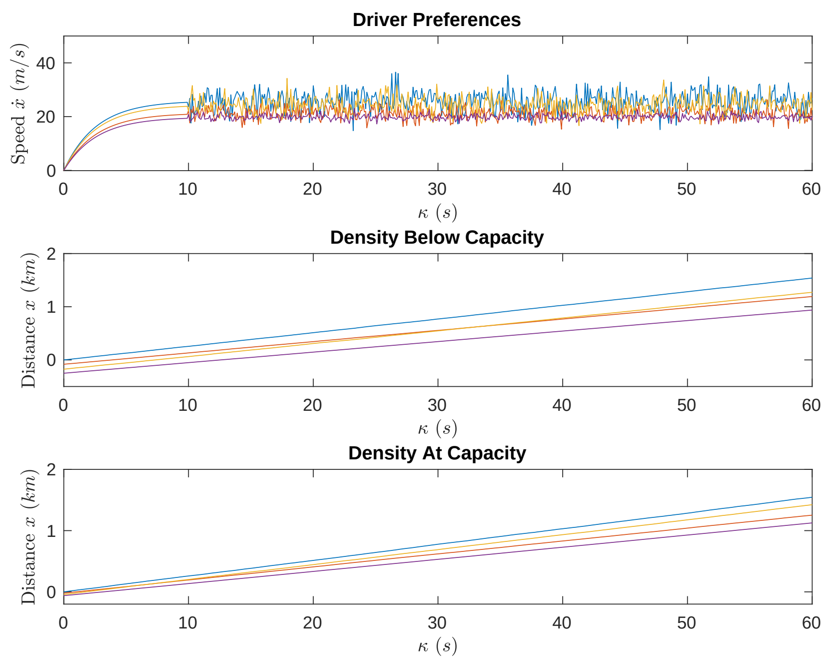

FIG. 2. Effects of vehicle arrival order, vehicle spacing and drivers on speed and travel distance.

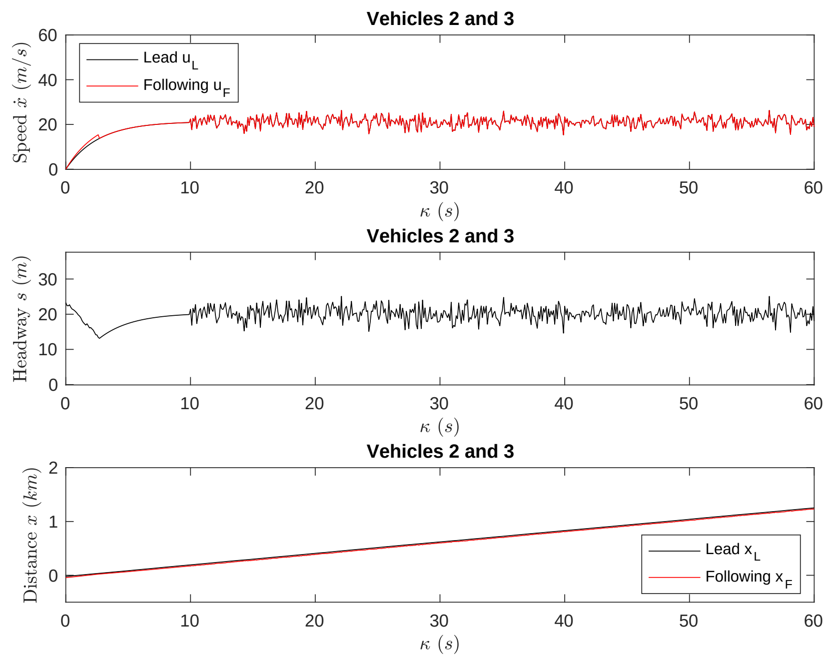

FIG. 3. Car-following effects on speed, headway and travel distance.

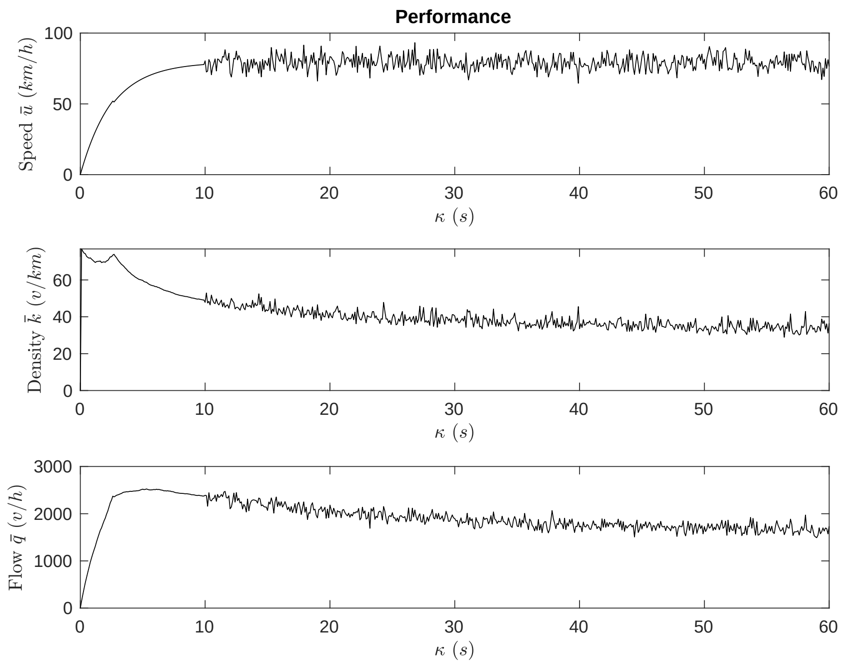

FIG. 4. "Ring-road" experiment traffic performance estimates.

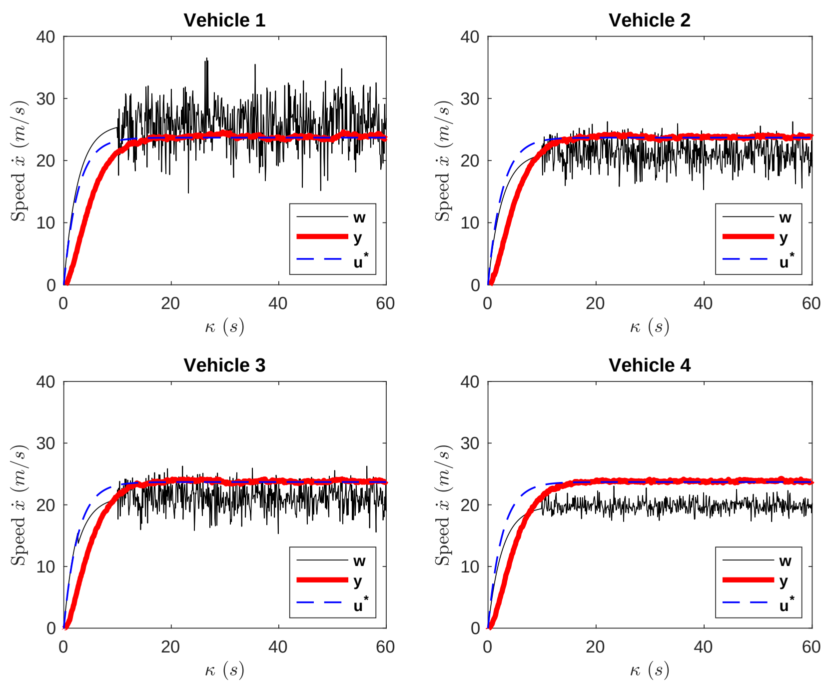

FIG. 5. Effects of controlling speed with Kalman Filter feedback control.